

# The inhomogeneous kinematic wave traffic flow model as a resonant nonlinear system

December, 2000

**W.-L. Jin**

Department of Mathematics,  
University of California, Davis, California 95616

**H. M. Zhang**

Author for correspondence  
Department of Civil and Environmental Engineering,  
University of California, Davis, California 95616

## Abstract

The kinematic wave traffic flow model for an inhomogeneous road is studied as a resonant nonlinear system, where an additional conservation law is introduced to model time-invariant road inhomogeneities such as changes in grades or number of lanes. This resonant system has two families of waves, one of which is a standing wave originated at the inhomogeneity. The nature of these waves are examined and their time-space structures are studied under Riemann initial conditions and proper entropy conditions. Moreover, the system is solved numerically with Godunov's method, and the solutions are found to be consistent with those of Daganzo (1995) and Lebacque (1996) for the same initial conditions. Finally, the numerical approximation is applied to model traffic flow on a ring road with a bottleneck and the results conform to expectations.

## Introduction

The kinematic wave traffic flow model of LWR was introduced by Lighthill and Whitham (1955) and Richards (1956) for modeling dense traffic flow on crowded roads, where the evolution of density

$\rho(x, t)$  and flow-rate  $q(x, t)$  over time is described by equation,

$$\rho_t + q_x = 0. \tag{1}$$

This equation follows conservation of traffic that vehicles are neither generated nor destroyed on a road section with no entries and exits.

The conservation equation alone is not sufficient to describe traffic evolution, because it does not capture the unique character of vehicular flow—drivers slow down when their front spacing is reduced to affect safety. The LWR model addresses this issue by assuming a functional relationship between local flow-rate and density, i.e.,  $q = f(x, \rho)$ . This flow-density relation, also known as the fundamental diagram of traffic flow, is often assumed to be concave in  $\rho$  and is a function of the local characteristics of a road location, such as the number of lanes, curvature, grades, and speed limit, as well as vehicle and driver composition. When a piece of roadway is homogeneous; i.e., the aforementioned characteristics of the road are uniform throughout the road section, the fundamental diagram is invariant to location  $x$  and the LWR model becomes

$$\rho_t + f(\rho)_x = 0. \tag{2}$$

In contrast, if a section of a roadway is inhomogeneous, the LWR model is

$$\rho_t + f(x, \rho)_x = 0. \tag{3}$$

Here we introduce a more explicit notation, an inhomogeneity factor  $a(x)$ , into the flux function  $f(x, \rho)$  and obtain the following equivalent LWR model for an inhomogeneous road

$$\rho_t + f(a, \rho)_x = 0. \tag{4}$$

This equation is particularly suited for our later analysis of the LWR model for inhomogeneous roads (We shall hereafter call (2) the homogeneous LWR model and (4) the inhomogeneous LWR model).

Both the homogeneous and inhomogeneous LWR models have been studied by researchers and applied by practitioners in the transportation community. Note that the homogeneous version (2) is nothing more than a scalar conservation law. Therefore, its wave solutions exist and are unique under the so-called ‘‘Lax entropy condition’’ (Lax, 1972). These solutions are formed by basic solutions to the Riemann problem of (2), in which the initial conditions jump at a boundary and are constant both upstream and downstream of the jump spot. Nevertheless, because analytical solutions are difficult to obtain for (2) with arbitrary initial/boundary conditions, numerical solutions have to be computed in most cases. The most often used approximation of (2) is perhaps

that of Godunov. In the Godunov method, a roadway is partitioned into a number of cells; and the change of the number of vehicles in each cell during a time interval is the net inflow of vehicles from its boundaries. The rate of traffic flowing through a boundary is obtained by solving a Riemann problem at this boundary. Besides the Godunov method, there are other types of approximations of the homogeneous LWR model, and some of them are shown to be variants of Godunov’s method (Lebacque 1996).

In contrast to the well researched homogeneous LWR model, the inhomogeneous model is less studied and less understood. Of the few efforts to rigorously solve the inhomogeneous LWR model, the works of Daganzo (1995) and Lebacque (1996) should be mentioned. In his cell transmission model, Daganzo started with a discrete form of the conservation equation and suggested that the flow through a boundary connecting two cells of a homogeneous road is the minimum of the “sending flow” from the upstream cell and the “receiving flow” of the downstream cell. The “sending flow” is equal to the upstream flow-rate if the upstream traffic is undercritical (UC) or the capacity of the upstream section if the upstream traffic is overcritical (OC); on the other hand, the “receiving flow” is equal to the capacity of the downstream section if the downstream traffic is UC or the downstream flow-rate if the downstream traffic is OC. In the homogeneous case, the boundary flux computed from the “sending flow” and the “receiving flow” is the same as that computed from solutions of the associated Riemann problem. Since the definitions of “sending flow” and “receiving flow” can be extended to inhomogeneous sections, Daganzo’s method can also be applied to the inhomogeneous LWR model. Different from Daganzo, Lebacque started his method with the solution of the “generalized” Riemann problem for (3). In this work, Lebacque came up with some rules for solving the “generalized” Riemann problem. These rules play the same role as entropy conditions. Moreover, Lebacque found that the boundary flux obtained from solving the Riemann problem is consistent with that from Daganzo’s method, and he called Daganzo’s “sending flow” demand and “receiving flow” supply.

The methods of Daganzo and Lebacque are streamlined versions of Godunov’s method for the inhomogeneous LWR model. They hinge upon the definitions of the demand and supply functions, which can be obtained unambiguously when  $f(a, \rho)$  is unimodal. When  $f(a, \rho)$  has multiple local maximum, or when the traffic flow model is of higher order, it is yet to be determined if equivalent demand/supply functions exist. Thus, these two methods may not be applicable to solve the LWR model that has multiple critical points on its fundamental diagram, nor higher-order models of traffic flow, such as the Payne-Whitham (Payne, 1971; Whitham, 1974) model and Zhang’s (1998, 1999, 2000, 2001) model. Note that, however, these higher-order models for homogeneous roads can still be solved with Godunov’s method (Zhang, 2001).

In this paper, we present a new method for solving the Riemann problem for (4), which can be extended to solve higher-order models. By introducing an additional conservation law for  $a(x)$ , we consider the inhomogeneous LWR model as a resonant nonlinear system and study its properties (Section 1). We also solve the Riemann problem for (4) and show that the boundary flux at the location of the inhomogeneity is consistent with the one given by Lebacque and Daganzo for the same initial condition (Section 2). Finally, we demonstrate our method through solving an initial value problem on a ring road with a bottleneck, and draw some conclusions from our analyses.

## 1 Properties of the inhomogeneous LWR model as a resonant nonlinear system

Instead of directly study the inhomogeneous LWR model described by (4), we augment (4) into a system of conservation laws through the introduction of an additional conservation law  $a_t = 0$  for the inhomogeneity factor  $a(x)$ , which leads to

$$U_t + F(U)_x = 0, \quad (5)$$

where  $U = (a, \rho)$ ,  $F(U) = (0, f(a, \rho))$ ,  $x \in R, t \geq 0$ . Without loss of generality, we assume the inhomogeneity is the drop/increase of lanes at a particular location, and write the fundamental diagram as  $f(a, \rho) = \rho v_*(\frac{\rho}{a})$ , where  $v = v_*(\frac{\rho}{a})$  is the speed-density relation. The results obtained hereafter apply to other types of inhomogeneities, such as changes in grades.

The inhomogeneous LWR model (5) can be linearized as

$$U_t + \partial F(U)U_x = 0, \quad (6)$$

where the differential  $\partial F(U)$  of the flux vector  $F(U)$  is

$$\partial F = \begin{bmatrix} 0 & 0 \\ -\frac{\rho^2}{a^2}v'_*(\frac{\rho}{a}) & v_*(\frac{\rho}{a}) + \frac{\rho}{a}v'_*(\frac{\rho}{a}) \end{bmatrix}. \quad (7)$$

The two eigenvalues of  $\partial F$  are

$$\lambda_0 = 0, \quad \lambda_1 = v_*(\frac{\rho}{a}) + \frac{\rho}{a}v'_*(\frac{\rho}{a}). \quad (8)$$

The corresponding right eigenvectors are

$$\mathbf{R}_0 = \begin{bmatrix} v_*(\frac{\rho}{a}) + \frac{\rho}{a}v'_*(\frac{\rho}{a}) \\ (\frac{\rho}{a})^2v'_*(\frac{\rho}{a}) \end{bmatrix}, \quad \mathbf{R}_1 = \begin{bmatrix} 0 \\ 1 \end{bmatrix},$$

and the left eigenvector of  $\partial f / \partial \rho$  as  $\mathbf{l}_1 = 1$ .

System (5) is a non-strictly hyperbolic system, since it can happen that  $\lambda_1 = \lambda_0$ . We consider a traffic state  $U_* = (a_*, \rho_*)$  in this system as critical if

$$\lambda_1(U_*) = 0; \quad (9)$$

i.e., at critical states, the two wave speeds are the same and system (5) is singular. For a critical traffic state  $U_*$  we also have

$$\frac{\partial}{\partial \rho} \lambda_1(U_*) = f_{\rho\rho} < 0 \quad (10)$$

since flow-rate is concave in traffic density, and

$$\frac{\partial}{\partial a} f(U_*) = -\left(\frac{\rho}{a}\right)^2 v'_*\left(\frac{\rho}{a}\right)|_{U_*} = \frac{\rho}{a} v_*\left(\frac{\rho}{a}\right)|_{U_*} > 0. \quad (11)$$

A consequence of properties (10) and (11) is that the linearized system (6) at  $U_*$  has the following normal form

$$\begin{bmatrix} \delta a \\ \delta \rho \end{bmatrix}_t + \begin{bmatrix} 0 & 0 \\ 1 & 0 \end{bmatrix} \begin{bmatrix} \delta a \\ \delta \rho \end{bmatrix}_x = 0. \quad (12)$$

System (12) has the solution  $\delta \rho(x, t) = \delta a'(x)t + c$ , and the solution goes to infinity as  $t$  goes to infinity. Therefore (12) is a linear resonant system, and the original inhomogeneous LWR model (5) is a nonlinear resonant system.

For (5), the smooth curve  $\Gamma$  in  $U$ -space formed by all critical states  $U_*$  are named a transition curve. Therefore  $\Gamma$  is defined as

$$\Gamma = \{U | \lambda_1(U) = 0\}.$$

Since  $\lambda_1(U) = v_*\left(\frac{\rho}{a}\right) + \frac{\rho}{a} v'_*\left(\frac{\rho}{a}\right)$ , we obtain

$$\Gamma = \left\{ (a, \rho) \mid \frac{\rho}{a} = \alpha, \text{ where } \alpha \text{ uniquely solves } v_*(\alpha) + \alpha v'_*(\alpha) = 0 \right\}; \quad (13)$$

i.e., the transition curve for (5) is a straight line passing through the origin in  $U$ -space. In (13),  $\alpha$  is unique since  $f(a, \rho)$  is concave in  $\rho$ .

The entropy solutions to a nonlinear resonant system are different from those to a strictly hyperbolic system of conservation laws. Isaacson and Temple (1992) proved that solutions to the Riemann problem for system (5) exist and are unique with the conditions (9)-(11). Lin, Temple and Wang (1995) presented solutions to a scalar nonlinear resonant system, which is similar to our system (5) except that  $f$  is convex in their study. In the next section we apply those results to solve the Riemann problem for the inhomogeneous LWR model.

## 2 Solutions to the Riemann problem

In this section we study the wave solutions to the Riemann problem for (5) with the following jump initial conditions

$$U(x, t = 0) = \begin{cases} U_L & \text{if } x < 0 \\ U_R & \text{if } x > 0 \end{cases}, \quad (14)$$

where the initial values of  $U_L, U_R$  are constant. For computational purposes, we are interested in the average flux at the boundary  $x = 0$  over a time interval  $\Delta t$ , which is denoted by  $f_0^*$  and defined as

$$f_0^* = \frac{1}{\Delta t} \int_0^{\Delta t} f(U(x = 0, t)) dt. \quad (15)$$

The augmented inhomogeneous LWR model (5) has two families of basic wave solutions associated with the two eigenvalues. The solutions whose wave speed is  $\lambda_0$  are in the 0-family, and the waves are called 0-waves. Similarly the solutions whose wave speed is  $\lambda_1$  are in the 1-family, and the waves are called 1-waves. The 0-wave is also called a standing wave since its wave speed is always 0. The 1-wave solutions are determined by the solutions of the scalar conservation law  $\rho_t + f(\bar{a}, \rho)_x = 0$ , where  $\bar{a}$  is a constant. Corresponding to the two types of wave solutions, the integral curves of the right eigenvectors  $\mathbf{R}_0$  and  $\mathbf{R}_1$  in  $U$ -space are called 0- and 1-curves respectively. Hence the 0-curves are given by  $f(U) = \text{const}$ , and the 1-curves are given by  $a = \text{const}$ . A 0-curve, a 1-curve, and the transition curve  $\Gamma$  passing through a critical state  $U_*$  are shown in **Figure 1**, where  $a$  is set as the vertical axis and  $\rho$  the horizontal axis.

As shown in **Figure 1**, the 0-curve is convex, and the 1-curve is tangent to the 0-curve at the critical state  $U_*$ . The transition curve  $\Gamma$  intersects the 0- and 1-curves at  $U_*$ , and there is only one critical state on one 0-curve or 1-curve. For any point  $U$ , only one 0-curve and one 1-curve pass it. In **Figure 1**, the states left to the transition curve are undercritical (UC) since  $\rho/a < \alpha$ ; and the states right to the transition curve are overcritical (OC) since  $\rho/a > \alpha$ .

The wave solutions to the Riemann problem for (5) are combinations of basic 0-waves and 1-waves. Since (5) is a hyperbolic system of conservation law, its wave solutions must satisfy Lax's entropy condition that the waves from left (upstream) to right (downstream) should increase their wave speeds so that they don't cross each other. For (5) as a resonant nonlinear system, an additional entropy condition is introduced by Isaacson and Temple,

$$\text{The standing wave can NOT cross the transition curve } \Gamma. \quad (16)$$

This entropy condition is equivalent to saying that, relative to the apexes of the fundamental diagrams, traffic conditions upstream and downstream of inhomogeneities are on the same side. That is, they should be either both UC or both OC.

With the two entropy conditions, the solutions to the inhomogeneous LWR model exist and are unique. The wave solutions for UC left state  $U_L$  are shown in **Figure 2**, and those for OC left state  $U_L$  are shown in **Figure 3**.

In the remaining part of this section, we discuss wave solutions to the Riemann problem for (5), present the formula for the boundary flux  $f_0^*$  related to each type of solution, summarize our results and compare them with those found in literature.

## 2.1 Solutions of the boundary fluxes

When  $U_L = (a_L, \rho_L)$  is UC; i.e.,  $\rho_L/a_L < \alpha$ , where  $\alpha$  is defined in (13), we denote the special critical point on standing wave passing  $U_L$  as  $U_*$ . Thus, as shown in **Figure 2**, the  $U$ -space is partitioned into three regions by  $DU_*$ ,  $OU_*$  and  $U_*C$ , where  $DU_* = \{(a, \rho) | a = a_*, \rho < \rho_*\}$ ,  $OU_* = \Gamma \cap \{0 \leq \rho \leq \rho_*\}$  and  $U_*C = \{(a, \rho) | f(a, \rho) = f(U_L), \rho > \rho_*\}$ . Related to different positions of the right state  $U_R$  in the  $U$ -space, the Riemann problem for (5) with initial conditions (14) has the following four types of wave solutions. For each type of solutions we provide formula for calculating the associated boundary flux  $f_0^*$ .

Type 1 When  $U_R$  is in region  $ABU_LU_*DA$  shown in **Figure 2**; i.e.,

$$f(U_R) < f(U_*) = f(U_L), \quad \rho_R/a_R < \alpha \text{ and } a_R \geq a_*, \quad (17)$$

wave solutions to the Riemann problem are of type 1. These solutions consist of two basic waves with an intermediate state  $U_1 = (a_R, \rho_1 |_{f(a_R, \rho_1) = f(U_*) = f(U_L)})$ . Of these two waves, the left one  $(U_L, U_1)$  is a standing wave, and the right one  $(U_1, U_R)$  is a rarefaction wave with characteristic velocity  $\lambda_1(a, \rho) > 0$ .

From **Figure 2**, we can see that the Riemann problem may admit this type of solutions when  $a_L > a_R$  or  $a_L \leq a_R$ ; i.e., when the road merges or diverges at  $x = 0$ . Here we present an example of this type of solutions in **Figure 4**, where the roadway merges at  $x = 0$ . In the case when the roadway diverges at  $x = 0$ , we can find similar solutions.

From **Figure 4**, we obtain the boundary flux  $f_0^* = f(U_L) = f(U_*)$  for wave solutions of type 1.

Type 2 When  $U_R$  is in region  $BU_LU_*CB$  shown in **Figure 2**; i.e.,

$$f(U_R) \geq f(U_*) = f(U_L), \quad (18)$$

wave solutions to the Riemann problem are of type 2. These solutions consist of two basic waves with an intermediate state  $U_1 = (a_R, \rho_1 |_{f(a_R, \rho_1) = f(U_*) = f(U_L)})$ . Of these two waves, the left  $(U_L, U_1)$  is a standing wave, and the right  $(U_1, U_R)$  is a shock wave with positive speed  $\sigma = \frac{f(U_R) - f(U_*)}{\rho_R - \rho_1} > 0$ .

From **Figure 2**, we can see that the Riemann problem may admit this type of solutions when the downstream traffic condition  $U_R$  is UC or OC, or the roadway merges or diverges at  $x = 0$ . Here we present an example of this type of solutions in **Figure 5**, where the downstream traffic condition is OC and the roadway merges at  $x = 0$ . Similar solutions can be found for other situations that satisfy (18).

From **Figure 5**, we obtain the boundary flux  $f_0^* = f(U_L) = f(U_*)$  for wave solutions of type 2. Here we have the same formula as that for wave solutions of type 1.

Type 3 When  $U_R$  is in region  $OU_*CO$  shown in **Figure 2**; i.e.,

$$f(U_R) < f(U_*) = f(U_L), \quad \rho_R/a_R \geq \alpha, \quad (19)$$

wave solutions to the Riemann problem are of type 3. These solutions consist of two basic waves with an intermediate state  $U_1 = (a_L, \rho_1 |_{f(a_L, \rho_1) = f(U_R)})$ . Of these two waves, the left one  $(U_L, U_1)$  is a shock wave with negative speed  $\sigma = \frac{f(U_1) - f(U_L)}{\rho_1 - \rho_L} < 0$ , and the right one  $(U_1, U_R)$  is a standing wave.

From **Figure 2**, we can see that the Riemann problem may admit this type of solutions when the roadway merges or diverges at  $x = 0$ . Here we present an example of this type of solutions in **Figure 6**, where the roadway merges at  $x = 0$ . In the case when the roadway diverges at  $x = 0$ , similar solutions can be found.

From **Figure 6**, we obtain the boundary flux  $f_0^* = f(U_R)$  for wave solutions of type 3.

Type 4 When  $U_R$  is in region  $OU_*DO$  shown in **Figure 2**; i.e.,

$$f(U_R) < f(U_*) = f(U_L), \quad \rho_R/a_R < \rho_*/a_* \text{ and } a_R < a_*, \quad (20)$$

wave solutions to the Riemann problem are of type 4. These solutions consist of three basic waves with two intermediate states:  $U_1 = (a_L, \rho_1 |_{f(a_L, \rho_1) = f(U_2)})$  and  $U_2 = (a_R, \rho_2 |_{\rho_2/a_R = \alpha})$ . Of these three waves, the left one  $(U_L, U_1)$  is a shock wave with negative speed  $\sigma = \frac{f(U_1) - f(U_L)}{\rho_1 - \rho_L} < 0$ .

0, the middle one  $(U_1, U_2)$  is a standing wave with zero speed, and the right one  $(U_2, U_R)$  is a rarefaction wave with characteristic velocity  $\lambda_1(a, \rho) > 0$ .

From **Figure 2**, we can see that this type of solutions are admitted only when the roadway merges at  $x = 0$ . Here we present an example of this type of solutions in **Figure 7**.

From **Figure 7**, we obtain the boundary flux  $f_0^* = f(U_2)$  for wave solutions of type 4.

When  $U_L = (a_L, \rho_L)$  is OC; i.e.,  $\rho_L/a_L > \alpha$ , we denote the special critical point on 1-wave curve passing  $U_L$  as  $U_*$ ; i.e.,  $U_* = (a_*, \rho_* |_{\rho_*/a_L = \alpha})$ . Thus, as shown in **Figure 3**, the  $U$ -space is partitioned into three regions by three curves  $DU_* = \{a = a_* = a_L, 0 \leq \rho \leq \rho_*\}$ ,  $OU_* = \{0 \leq a \leq a_*, \rho = a\alpha\}$  and  $U_*C = \{a \geq a_*, f(a, \rho) = f(U_*)\}$ . Related to different positions of the right state  $U_R$  in the  $U$ -space, the Riemann problem for (5) with initial conditions (14) has the following six types of wave solutions. For each type of solutions we provide formula for calculating the associated boundary flux  $f_0^*$ .

Type 5 When  $U_R$  resides in region  $ABU_*DA$  shown in **Figure 3**; i.e.,

$$f(U_R) < f(U_*), \quad \rho_R/a_R < \alpha \text{ and } a_R \geq a_* = a_L, \quad (21)$$

wave solutions to the Riemann problem are of type 5. These solutions consist of three basic waves with two intermediate states:  $U_1 = U_*$  and  $U_2 = (a_R, \rho_2 |_{f(U_2)=f(U_*)})$ . Of these three waves, the left one  $(U_L, U_1)$  is a rarefaction wave with negative characteristic wave velocity  $\lambda_1(a, \rho)$ , the middle one  $(U_1, U_2)$  is a standing wave and the right one  $(U_2, U_R)$  is a rarefaction wave with positive characteristic velocity  $\lambda_1(a, \rho)$ .

From **Figure 3**, we can see that this type of solutions are admitted only when the roadway diverges at  $x = 0$ . Here we present an example of this type of solutions in **Figure 8**.

From **Figure 8**, we obtain the boundary flux  $f_0^* = f(U_2)$  for wave solutions of type 5.

Type 6 When  $U_R$  resides in region  $BU_*CB$  shown in **Figure 3**; i.e.,

$$f(U_R) \geq f(U_*), \quad (22)$$

solutions to the Riemann problem are of type 6. These solutions consist of three basic waves with two intermediate states:  $U_1 = U_*$  and  $U_2 = (a_R, \rho_2 |_{f(U_2)=f(U_*)})$ . Of these three waves, the left one  $(U_L, U_1)$  is a rarefaction wave with negative characteristic velocity  $\lambda_1(a, \rho)$ , the middle one  $(U_1, U_2)$  is a standing wave and the right one  $(U_2, U_R)$  is a shock wave with positive speed  $\sigma = \frac{f(U_R) - f(U_2)}{\rho_R - \rho_2}$ .

From **Figure 3**, we can see that this type of solutions may be admitted when the downstream traffic condition is UC or OC; However, they are admitted only when the roadway diverges at  $x = 0$ . Here we present an example of this type of solutions in **Figure 9**, where the downstream traffic condition is OC. In the case when the downstream traffic condition is UC, we can find similar solutions.

From **Figure 9**, we obtain the boundary flux  $f_0^* = f(U_2)$  for this type of wave solutions. Here we have the same formula as that for wave solutions of type 5.

Type 7 When  $U_R$  resides in region  $CU_*FU_L EC$  shown in **Figure 3**; i.e.,

$$f(U_L) \leq f(U_R) < f(U_*) \text{ and } \rho_R/a_R \geq \alpha, \quad (23)$$

wave solutions to the Riemann problem are of type 7. These solutions consist of two basic waves with an intermediate state  $U_1 = (a_L, \rho_1|_{f(U_1)=f(U_R)})$ . Of these two waves, the left one  $(U_L, U_1)$  is a rarefaction with negative characteristic velocity  $\lambda_1(a, \rho)$ , and the right one  $(U_1, U_R)$  is a standing wave.

From **Figure 3**, we can see that the Riemann problem may admit this type of solutions when the roadway merges or diverges at  $x = 0$ . Here we present an example of this type of solutions in **Figure 10**, where the roadway diverges at  $x = 0$ . In the case when the roadway merges, we can find similar solutions.

From **Figure 10**, we obtain the boundary flux  $f_0^* = f(U_R)$  for wave solutions of type 7.

Type 8 When  $U_R$  locates in region  $FU_L EOF$  shown in **Figure 3**; i.e.,

$$f(U_R) < f(U_L) < f(U_*) \text{ and } \rho_R/a_R \geq \alpha, \quad (24)$$

wave solutions to the Riemann problem are of type 8. These solutions consist of two basic waves with an intermediate state  $U_1 = (a_L, \rho_1|_{f(U_1)=f(U_R)})$ . Of these two waves, the left one  $(U_L, U_1)$  is a shock with negative speed  $\sigma = \frac{f(U_L)-f(U_1)}{\rho_L-\rho_1}$ , and the right one  $(U_1, U_R)$  is a standing wave.

Like in the previous case, the Riemann problem may admit this type of solutions when the roadway merges or diverges at  $x = 0$ . Here we present an example of this type of solutions in **Figure 11**, where the roadway diverges at  $x = 0$ . In the case when the roadway merges, we can find similar solutions.

From **Figure 11**, we obtain the boundary flux  $f_0^* = f(U_R)$  for wave solutions of type 8. The formula is the same as that for wave solutions of type 7.

Type 9 When  $U_R$  resides in region  $DU_*FGD$  shown in **Figure 3**; i.e.,

$$f(U_L) \leq f(U_R) < f(U_*), \quad \rho_R/a_R < \alpha \text{ and } a_R < a_* = a_L, \quad (25)$$

wave solutions to the Riemann problem are of type 9. These solutions consist of three basic waves with two intermediate states:  $U_1 = (a_L, \rho_1|_{f(U_1)=f(U_2)})$  and  $U_2 = (a_R, \rho_2|_{\rho_2/a_R=\alpha})$ . Of these three waves, the left one  $(U_L, U_1)$  is a rarefaction with negative characteristic velocity  $\lambda_1(a, \rho)$ , the middle one  $(U_1, U_2)$  is a standing wave, and the right one  $(U_2, U_R)$  is a rarefaction with positive speed  $\lambda_1(a, \rho)$ .

From **Figure 3**, we can see that this type of solutions are admitted only when the roadway merges at  $x = 0$ . Here we present an example of this type of solutions in **Figure 12**.

From **Figure 12**, we obtain the boundary flux  $f_0^* = f(U_2)$  for wave solutions of type 9.

Type 10 When  $U_R$  resides in region  $GFOG$  shown in **Figure 3**; i.e.,

$$f(U_R) < f(U_L) < f(U_*), \quad \rho_R/a_R < \alpha \text{ and } a_R < a_* = a_L, \quad (26)$$

wave solutions to the Riemann problem are of type 10. These solutions consist of three basic waves with two intermediate states:  $U_1 = (a_L, \rho_1|_{f(U_1)=f(U_2)})$  and  $U_2 = (a_R, \rho_2|_{\rho_2/a_R=\alpha})$ . Of these three waves, the left one  $(U_L, U_1)$  is a shock with negative speed, the middle one  $(U_1, U_2)$  is a standing wave, and the right one  $(U_2, U_R)$  is a rarefaction wave with positive characteristic velocity  $\lambda_1(a, \rho)$ .

Like in the previous case, this type of solutions are admitted only when the roadway merges at  $x = 0$ . Here we present an example of this type of solutions in **Figure 13**.

From **Figure 13**, we obtain the boundary flux  $f_0^* = f(U_2)$  for wave solutions of type 10. Here we have the same formula as that for wave solutions of type 9.

## 2.2 Summary

In each of the 10 cases discussed above, the boundary flux  $f_0^*$  is equal to one of the following four quantities: the upstream flow-rate  $f(U_L)$ , the downstream flow-rate  $f(U_R)$ , the capacity of the upstream roadway  $f_L^{max}$  and the capacity of the downstream roadway  $f_R^{max}$ . For wave solutions of type 1 and 2, the boundary flux is equal to the upstream traffic flow-rate; i.e.,  $f_0^* = f(U_L)$ . For wave solutions of type 3, 7 and 8, the boundary flux is equal to the downstream traffic flow-rate; i.e.,  $f_0^* = f(U_R)$ . For wave solutions of type 4, 9 and 10, the boundary flux is equal to the capacity of the downstream roadway; i.e.,  $f_0^* = f_R^{max}$ . For wave solutions of type 5 and 6, the boundary flux

is equal to the capacity of the upstream roadway; i.e.,  $f_0^* = f_L^{max}$ . In Table 1, the boundary fluxes are listed for the 10 types of wave solutions to the Riemann problem, as well as the conditions when the Riemann problem admit those solutions.

Note that when  $a_L = a_R$ ; i.e., when (4) becomes a homogeneous LWR model, wave solutions and the solutions of the boundary fluxes provided here are the same as those for the homogeneous LWR model.

Lebacque (1996) studied the Riemann problem of the inhomogeneous LWR for (3). He classified the problem according to two criteria. The first criterion is to compare capacity of the upstream cell and that of the downstream cell. For the roadway with variable number of lanes, it is equivalently to compare the number of lanes of the upstream cell and that of the downstream cell. The second criterion is to consider whether the upstream and downstream traffic conditions are UC or OC. With these criteria, he discussed 8 types of waves solutions to the Riemann problem and obtained the formula for the boundary flux related to each type of solutions. The conditions for those types of wave solutions as well as the formulas related to those types of solutions are listed in Table 2. Under each of those conditions, the Riemann problem may admit different types of solutions discussed in Section 2.1. The types of solutions and our related formulas for the boundary flux are also presented in Table 2. From this table, we can see that our results are consistent with those provided by Lebacque, although the Riemann problem is solved through different approaches.

The consistency of our results with existing results can also be shown by introducing a simple formula for the boundary flux. If we define the upstream demand as

$$f_L^* = \begin{cases} f(U_L), & \rho_L/a_L < \alpha \\ f_L^{max}, & \rho_L/a_L \geq \alpha \end{cases} \quad (27)$$

and define the downstream supply as

$$f_R^* = \begin{cases} f_R^{max}, & \rho_R/a_R < \alpha \\ f(U_R), & \rho_R/a_R \geq \alpha \end{cases} \quad (28)$$

then the boundary flux can be simply computed as

$$f_0^* = \min\{f_L^*, f_R^*\}. \quad (29)$$

Note that  $f_L^* = f(U_*)$ . Formula (29) was also provided by Daganzo (1995) and Lebacque (1996).

### 3 Simulation of traffic flow on a ring road with a bottleneck

#### 3.1 Solution method

The augmented inhomogeneous LWR model, expressed in conservation form (5), can be solved efficiently with Godunov's method under general initial and boundary conditions. In Godunov's method, the roadway is partitioned into  $N$  cells and a duration of time is discretized into  $M$  time steps. In a cell  $i$ , we approximate the continuous equation (5) with a finite difference equation

$$\frac{U_i^{m+1} - U_i^m}{\Delta t} + \frac{F_{i-1/2}^* - F_{i+1/2}^*}{\Delta x} = 0, \quad (30)$$

whose component for  $\rho$  is

$$\frac{\rho_i^{m+1} - \rho_i^m}{\Delta t} + \frac{f_{i-1/2}^* - f_{i+1/2}^*}{\Delta x} = 0, \quad (31)$$

where  $\rho_i^m$  denotes the average of  $\rho$  in cell  $i$  at time step  $m$ , similarly  $\rho_i^{m+1}$  is the average at time step  $m+1$ ;  $f_{i-1/2}^*$  denotes the flux through the upstream boundary of cell  $i$ , and similarly  $f_{i+1/2}^*$  denotes the downstream boundary flux of cell  $i$ . In (31), the boundary flux  $f_{i-1/2}^*$  is related to solutions to a Riemann problem for (5) with the following initial conditions:

$$U(x = x_{i-1/2}, t = t_m) = \begin{cases} U_{i-1}^m & x < x_{i-1/2} \\ U_i^m & x > x_{i-1/2} \end{cases}, \quad (32)$$

which have been discussed in Section 2.

#### 3.2 Numerical results

We use the approximation developed earlier to simulate traffic on a ring road. The length of the ring road is  $L = 800l = 22.4$  km. The simulation time is  $T = 500\tau = 2500$  s = 41.7 min. We partition the road  $[0, L]$  into  $N = 100$  cells and the time interval  $[0, T]$  into  $K = 500$  steps. Hence, the length of each cell is  $\Delta x = 0.224$  km and the length of each time step is  $\Delta t = 5$  s. Since  $|\lambda_*| \leq v_f = 5l/\tau$ , we find the CFL (Courant-Friedrichs-Lewy, 1928) condition number

$$\max |\lambda_*| \frac{\Delta t}{\Delta x} \leq 0.625 < 1.$$

Moreover, we adopt in this simulation the fundamental diagram used in (Kerner and Konhäuser, 1994; Herrmann and Kerner, 1998) with the following parameters: the relaxation time  $\tau = 5$  s; the unit length  $l = 0.028$  km; the free flow speed  $v_f = 5.0l/\tau = 0.028$  km/s = 100.8 km/h; the

jam density of a single lane  $\rho_j = 180$  veh/km/lane. The equilibrium speed-density relationship is therefore

$$v_*(\rho, a(x)) = 5.0461 \left[ \left( 1 + \exp\left\{ \left[ \frac{\rho}{a(x)\rho_j} - 0.25 \right] / 0.06 \right\} \right)^{-1} - 3.72 \times 10^{-6} \right] l/\tau,$$

where  $a(x)$  is the number of lanes at location  $x$ . The equilibrium functions  $v_*(\rho, a(x))$  and  $f(\rho, a(x))$  are given in **Figure 14**.

The first simulation is about the homogeneous LWR model. Here we assume that the ring road has single lane everywhere; i.e.,  $a(x) = 1$  for any  $x \in [0, L]$ , and use a global perturbation as the initial condition

$$\begin{aligned} \rho(x, 0) &= \rho_h + \Delta\rho_0 \sin \frac{2\pi x}{L}, & x \in [0, L], \\ v(x, 0) &= v_*(\rho(x, 0), 1), & x \in [0, L], \end{aligned} \quad (33)$$

with  $\rho_h = 28$  veh/km and  $\Delta\rho_0 = 3$  veh/km (the corresponding initial condition (33) is depicted in **Figure 15**).

The results are shown in **Figure 16**, from which we observe that initially wave interactions are strong but gradually the bulge sharpens from behind and expands from front to form a so-called *N*-wave that travels around the ring with a nearly fixed profile.

In the second simulation we created a bottleneck on the ring road with the following lane configuration:

$$a(x) = \begin{cases} 1, & x \in [320l, 400l], \\ 2, & \text{elsewhere} . \end{cases} \quad (34)$$

As before, we also use a global perturbation as the initial condition

$$\begin{aligned} \rho(x, 0) &= a(x)(\rho_h + \Delta\rho_0 \sin \frac{2\pi x}{L}), & x \in [0, L], \\ v(x, 0) &= v_*(\rho(x, 0), a(x)), & x \in [0, L], \end{aligned} \quad (35)$$

with  $\rho_h = 28$  veh/km/lane and  $\Delta\rho_0 = 3$  veh/km/lane (the corresponding initial condition (35) is depicted in **Figure 17**).

The results for this simulation are shown in **Figure 18**, and are more interesting. We observe from this figure that at first flow increases in the bottleneck to make the bottleneck saturated, then a queue forms upstream of the bottleneck, whose tail propagates upstream as a shock. At the same time, traffic emerging from the bottleneck accelerates in an expansion wave. After a while, all the commotion settles and an equilibrium state is reached, where a stationary queue forms upstream of the bottleneck, whose in/out flux equals the capacity of the bottleneck. Similar

situations can be observed in real world bottlenecks, although queues formed at such bottlenecks rarely reach equilibrium because, unlike in the ring road example, their traffic demands change over time. Therefore, we observe queues forming, growing, and dissipating at locations with lane drops, upward slopes, or tight turns. Sometimes queues formed at a bottleneck can grow fairly long, to the extent that they entrap vehicles that do not use the bottleneck. Under such situations, we can implement various types of control strategies, such as ramp metering, to control the extent of the bottleneck queues so that they do not block vehicles that wish to exit upstream of the bottleneck. For this purpose the numerical method presented here can be used to help model and design effective control.

## 4 Concluding remarks

We studied the inhomogeneous LWR model as a nonlinear resonant system. The nonlinear resonance arises when the two characteristics of the augmented LWR model coalesce. Critical states and a transitional curve  $\Gamma$  can be defined in the  $U$  space based on the behavior of these characteristics, which are in turn used to solve the Riemann problem for the inhomogeneous LWR model. It is found that, under the entropy conditions of Lax and of Isaacson and Temple, there exist ten types of wave solutions. Formulas for computing the boundary fluxes related to different types of wave solutions were also obtained. These formulas, after translated into the supply/demand framework, are found to be consistent with those found in literature. For problems with general initial/boundary conditions, the method of Godunov was applied to solve the inhomogeneous model numerically.

The method presented here can be extended easily to model more complicated situations, such as multiple inhomogeneities. Suppose at location  $x$ , there are  $i = 1, \dots, n$  types of inhomogeneities, such as changes in number of lanes, grade, and curvature. We introduce an inhomogeneity vector  $\vec{a}(x) = (a_1(x), a_2(x), \dots, a_n(x))^T$ , and express the flow-density function as  $f(\vec{a}(x), \rho)$ . Then the conservation law becomes

$$\begin{cases} \rho_t + f(\vec{a}(x), \rho)_x & = 0, \\ \vec{a}(x)_t & = 0, \end{cases}$$

and this higher-dimensional nonlinear resonant system can be solved in a similar way. It is worth mentioning that the augmentation approach taken in this paper also applies to higher-order traffic flow models for inhomogeneous roads.

## Acknowledgements

We thank Dr. John M. Hong for several stimulating discussions and suggestion of two key references. A CAREER grant from the National Science Foundation is also acknowledged.

## References

- [1] Courant, R., Friedrichs, K., and Lewy, H. (1928). ber die partiellen differenzengleichungen der mathematischen physik. *Mathematische Annalen*, 100:32–74.
- [2] Daganzo, C. F. (1995). The cell transmission model II: Network traffic. *Transportation Research B*, 29(2):79–93.
- [3] Isaacson, E. I. and Temple, J. B. (1992). Nonlinear resonance in systems of conservation laws. *SIAM Journal on Applied Mathematics*, 52(5):1260–1278.
- [4] Lax, P. D. (1972). *Hyperbolic systems of conservation laws and the mathematical theory of shock waves*. SIAM, Philadelphia, Pennsylvania.
- [5] Lebacque, J. P. (1996). The godunov scheme and what it means for first order traffic flow models. In *The International Symposium on Transportation and Traffic Theory*, Lyon, France.
- [6] Lighthill, M. J. and Whitham, G. B. (1955). On kinematic waves: II. a theory of traffic flow on long crowded roads. *Proceedings of the Royal Society of London A*, 229:317–345.
- [7] Lin, L., Temple, J. B., and Wang, J. (1995). A comparison of convergence rates for godunov’s method and glimm’s method in resonant nonlinear systems of conservation laws. *SIAM Journal on Numerical Analysis*, 32(3):824–840.
- [8] Payne, H. J. (1971). Models of freeway traffic and control. In *Mathematical Models of Public Systems*, volume 1 of *Simulation Councils Proceeding Series*, pages 51–60.
- [9] Richards, P. I. (1956). Shock waves on the highway. *Operations Research*, 4:42–51.
- [10] Whitham, G. B. (1974). *Linear and nonlinear waves*. John Wiley and Sons, New York.
- [11] Zhang, H. M. (1998). A theory of nonequilibrium traffic flow. *Transportation Research B*, 32(7):485–498.

- [12] Zhang, H. M. (1999). An analysis of the stability and wave properties of a new continuum theory. *Transportation Research B*, 33(6):387–398.
- [13] Zhang, H. M. (2000). Structural properties of solutions arising from a non-equilibrium traffic flow theory. *Transportation Research B*, 34:583–603.
- [14] Zhang, H. M. (2001). A finite difference model of nonequilibrium traffic flow. *Transportation Research B*, 35(5):337–365.

No.	left state $U_L$	right state $U_R$	boundary flux $f_0^*$
1	UC	$f(U_R) < f(U_L), a_R > a_*, \rho_R/a_R < \alpha$	$f(U_L)$
2	UC	$f(U_R) > f(U_L)$	$f(U_L)$
3	UC	$f(U_R) < f(U_L), \rho_R/a_R > \alpha$	$f(U_R)$
4	UC	$f(U_R) < f(U_L), \rho_R/a_R < \alpha, a_R < a_*$	$f_R^{max}$
5	OC	$f(U_R) < f_L^{max}, a_R > a_L, \rho_R/a_R < \alpha$	$f_L^{max}$
6	OC	$f(U_R) > f_L^{max}$	$f_L^{max}$
7	OC	$f(U_L) < f(U_R) < f_L^{max}, \rho_R/a_R > \alpha$	$f(U_R)$
8	OC	$f(U_R) < f(U_L), \rho_R/a_R > \alpha$	$f(U_R)$
9	OC	$f(U_L) < f(U_R) < f_L^{max}, \rho_R/a_R < \alpha, a_R < a_L$	$f_R^{max}$
10	OC	$f(U_R) < f(U_L), \rho_R/a_R < \alpha, a_R < a_L$	$f_R^{max}$

Table 1: Solutions of the Boundary Fluxes

Conditions	Solutions by Lebacque	Types	Our solutions
$a_L \leq a_R, U_L \text{ UC}, U_R \text{ UC}$	$f(U_L)$	1	$f(U_L)$
$a_L \leq a_R, U_L \text{ UC}, U_R \text{ OC}$	$\min\{f(U_L), f(U_R)\}$	2 or 3	$f(U_L)$ or $f(U_R)$
$a_L \leq a_R, U_L \text{ OC}, U_R \text{ UC}$	$f_L^{max}$	5 or 6	$f_L^{max}$
$a_L \leq a_R, U_L \text{ OC}, U_R \text{ OC}$	$\min\{f_L^{max}, f(U_R)\}$	6, 7 or 8	$f_L^{max}$ or $f(U_R)$
$a_L \geq a_R, U_L \text{ UC}, U_R \text{ UC}$	$\min\{f_R^{max}, f(U_L)\}$	1 or 4	$f(U_L), f_R^{max}$
$a_L \geq a_R, U_L \text{ UC}, U_R \text{ OC}$	$\min\{f(U_L), f(U_R)\}$	2 or 3	$f(U_L)$ or $f(U_R)$
$a_L \geq a_R, U_L \text{ OC}, U_R \text{ UC}$	$f_R^{max}$	9 or 10	$f_R^{max}$
$a_L \geq a_R, U_L \text{ OC}, U_R \text{ OC}$	$f(U_R)$	7 or 8	$f(U_R)$

Table 2: Comparison with Lebacque's results

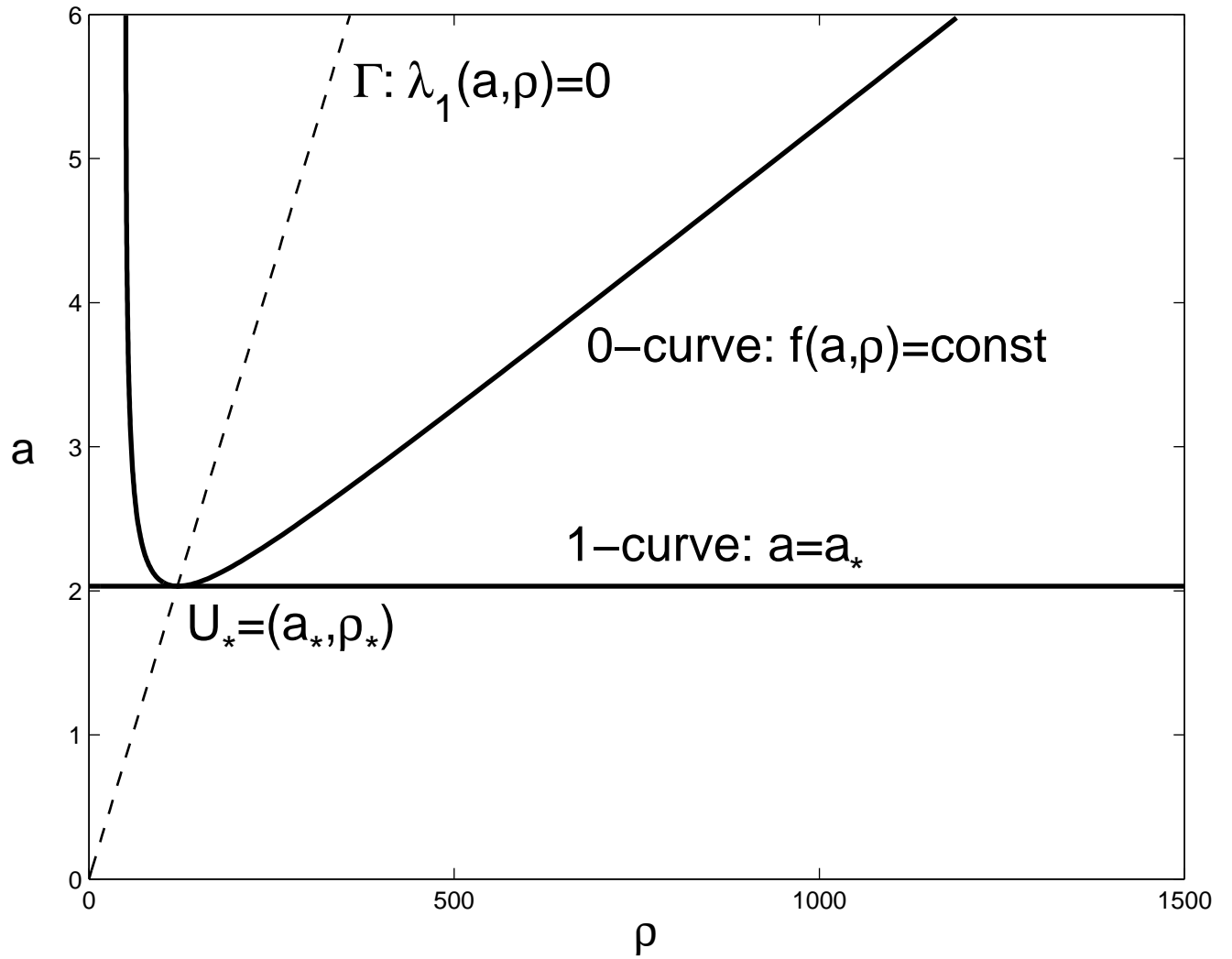


Figure 1: Integral curves



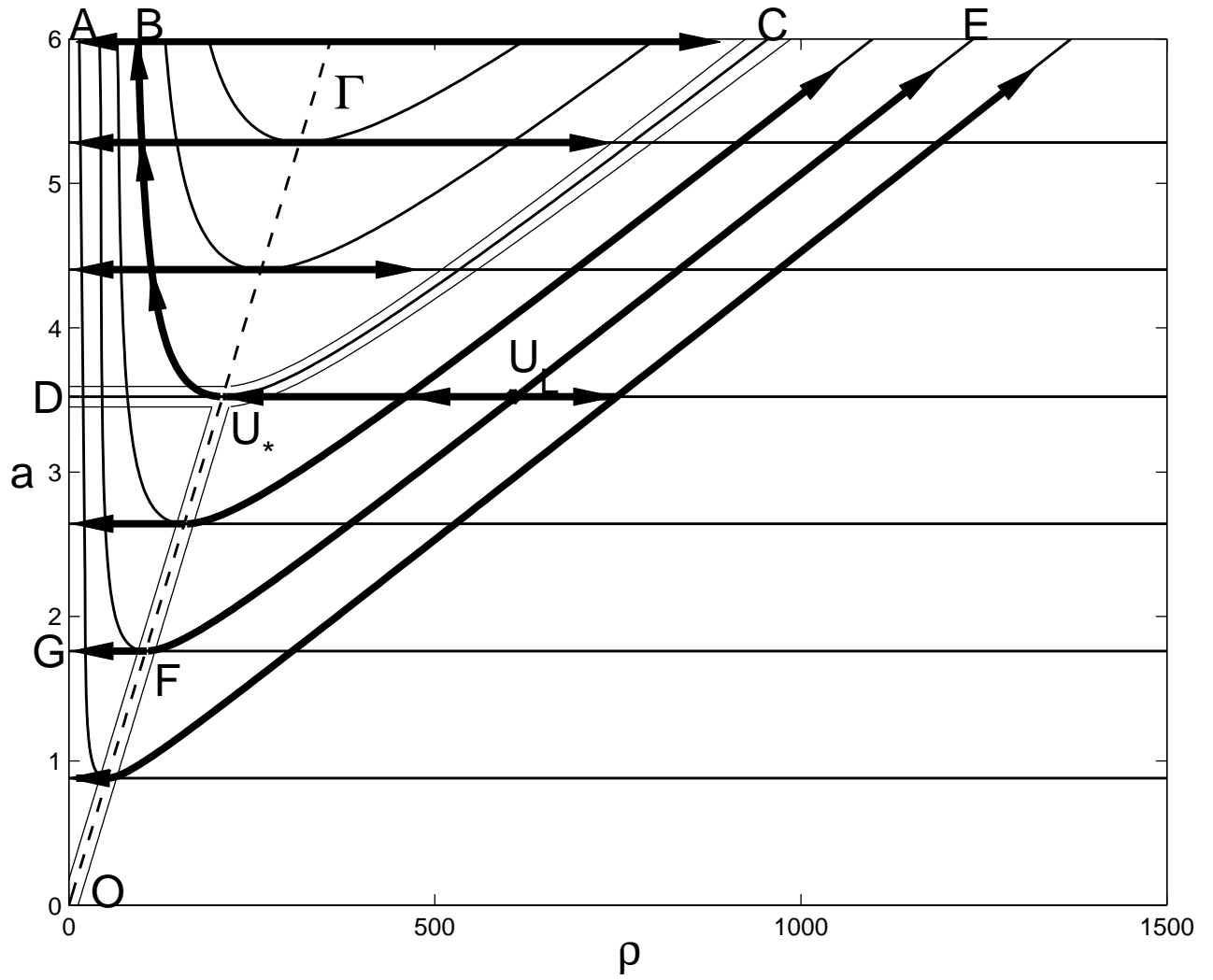


Figure 3: The Riemann problem for  $U_L$  right of  $\Gamma$

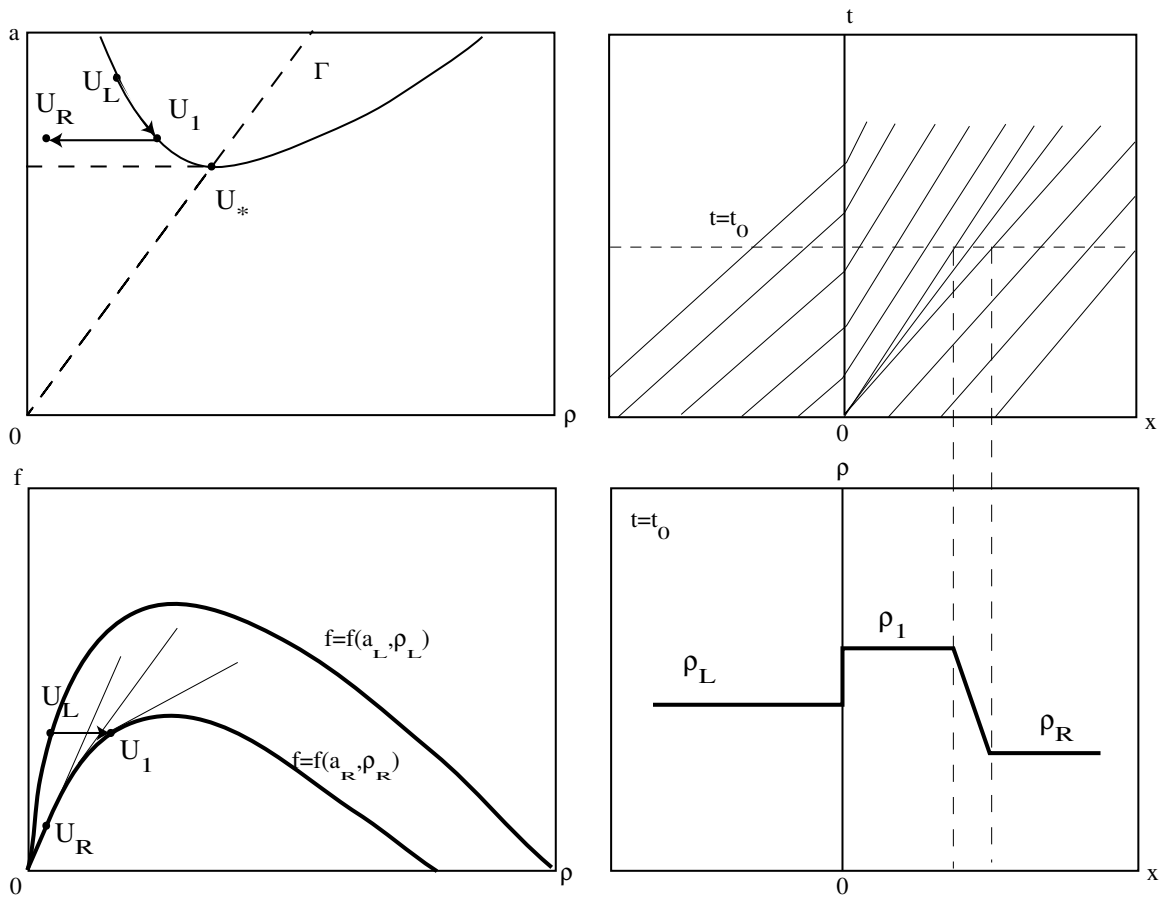


Figure 4: An example for wave solutions of type 1 for (5) with initial conditions (14)

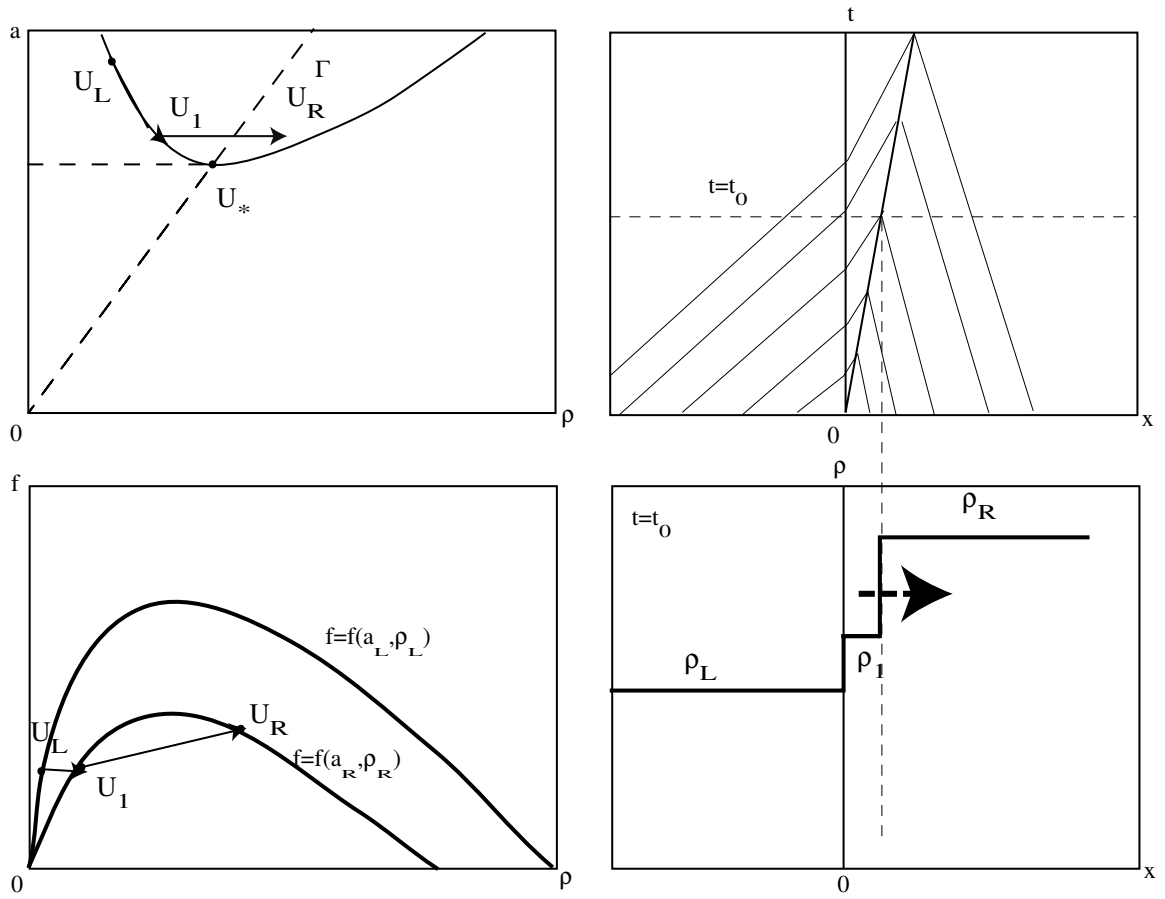


Figure 5: An example for wave solutions of type 2 for (5) with initial conditions (14)

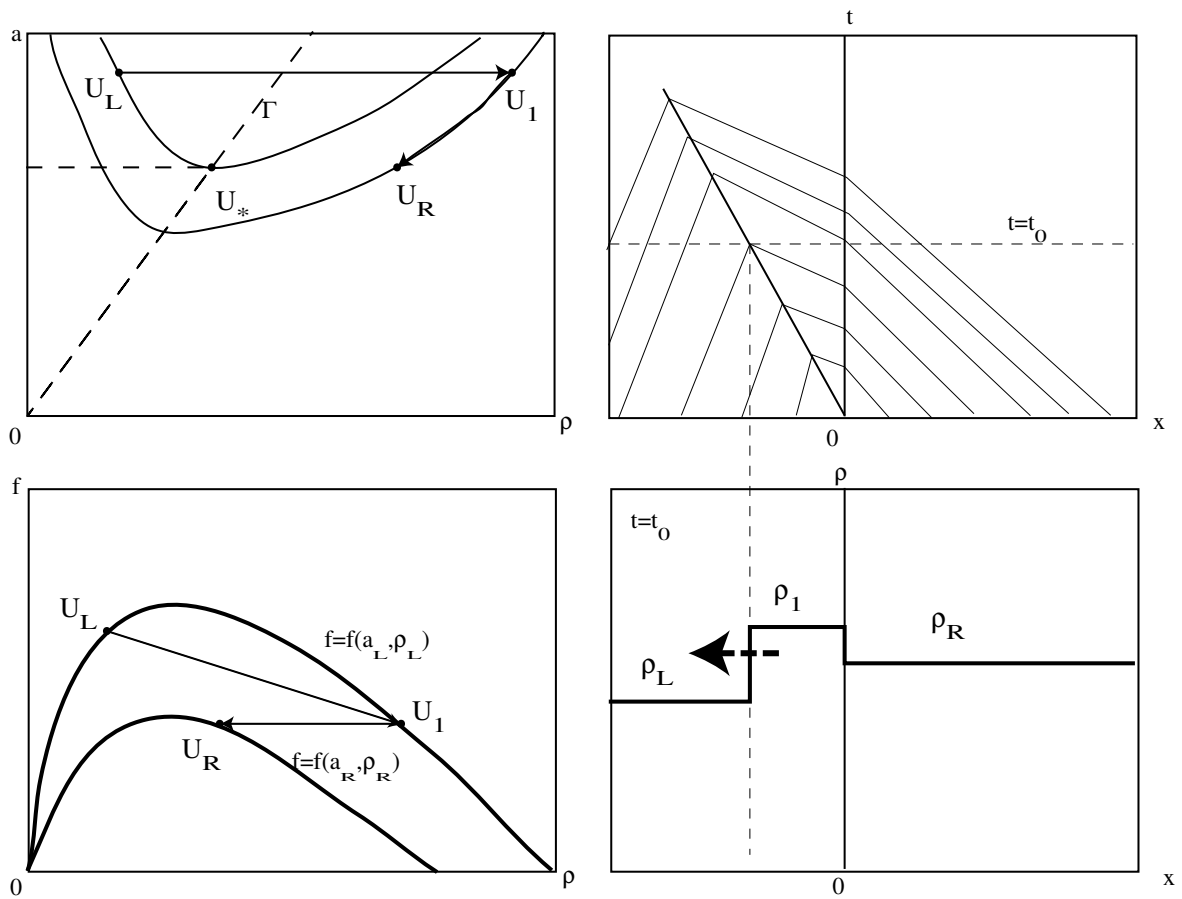


Figure 6: An example for wave solutions of type 3 for (5) with initial conditions (14)

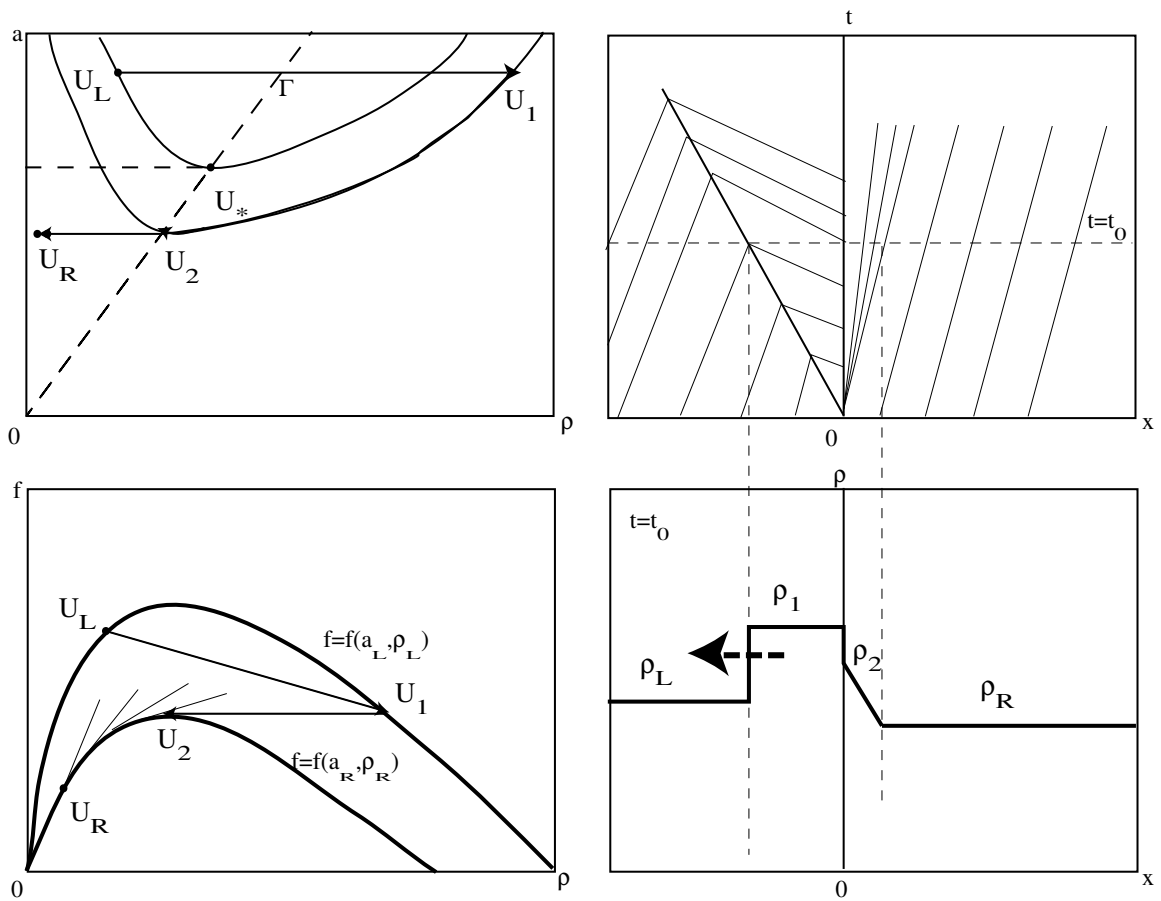


Figure 7: An example for wave solutions of type 4 for (5) with initial conditions (14)

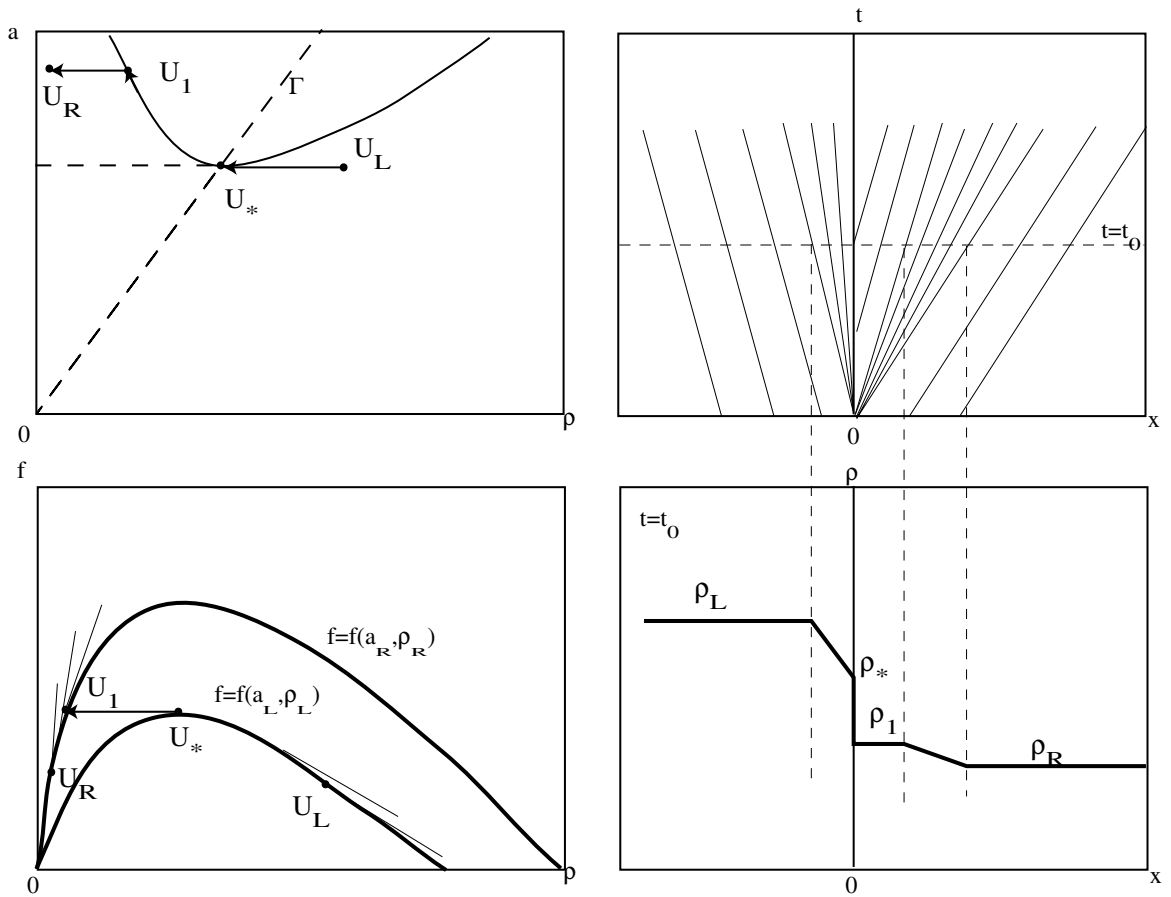


Figure 8: An example for wave solutions of type 5 for (5) with initial conditions (14)

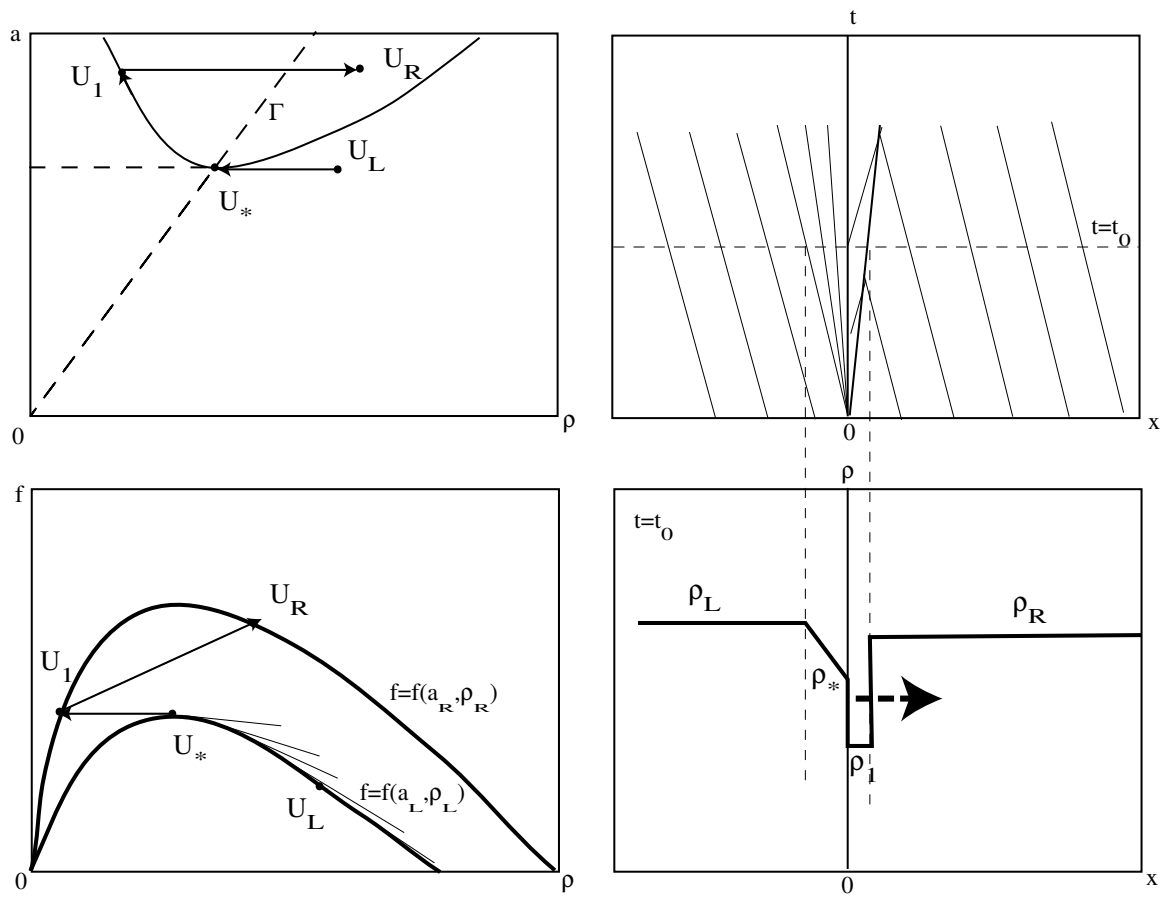


Figure 9: An example for wave solutions of type 6 for (5) with initial conditions (14)

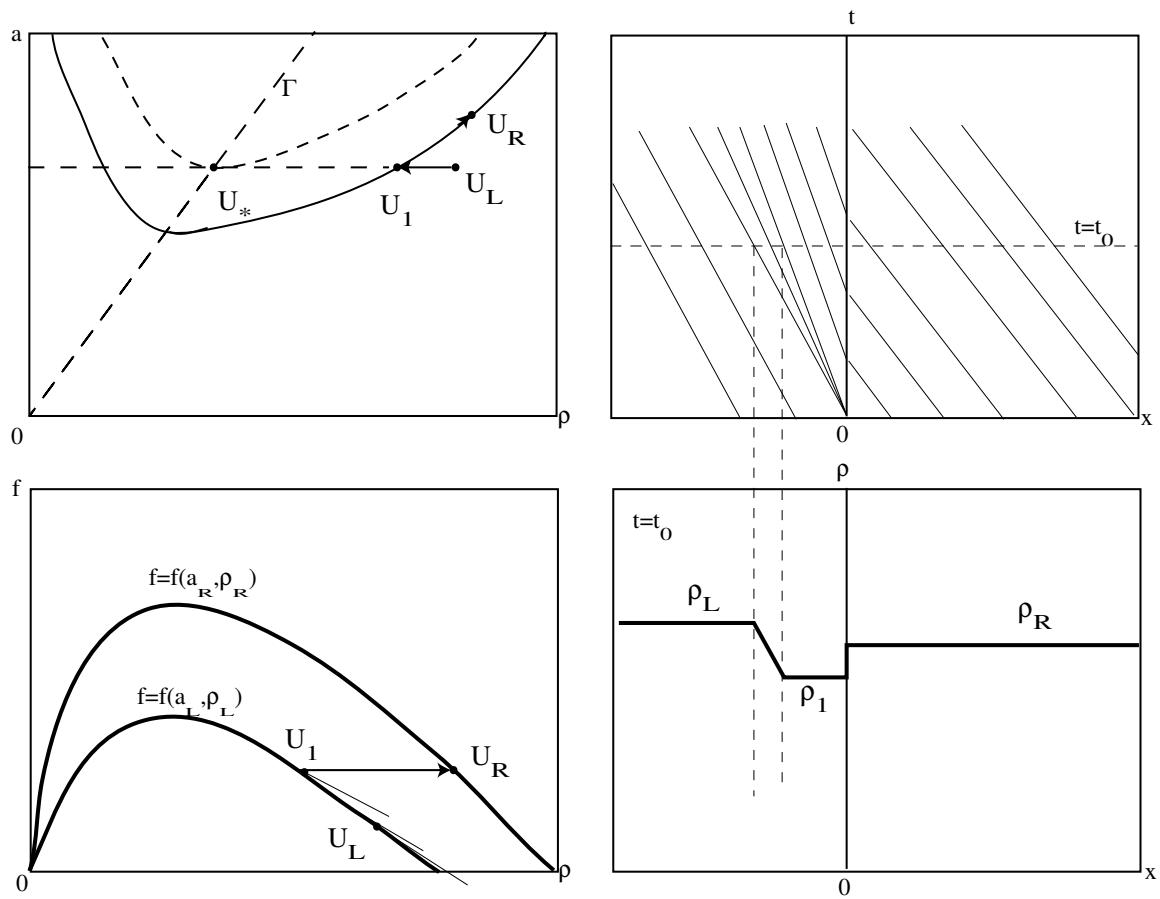


Figure 10: An example for wave solutions of type 7 for (5) with initial conditions (14)

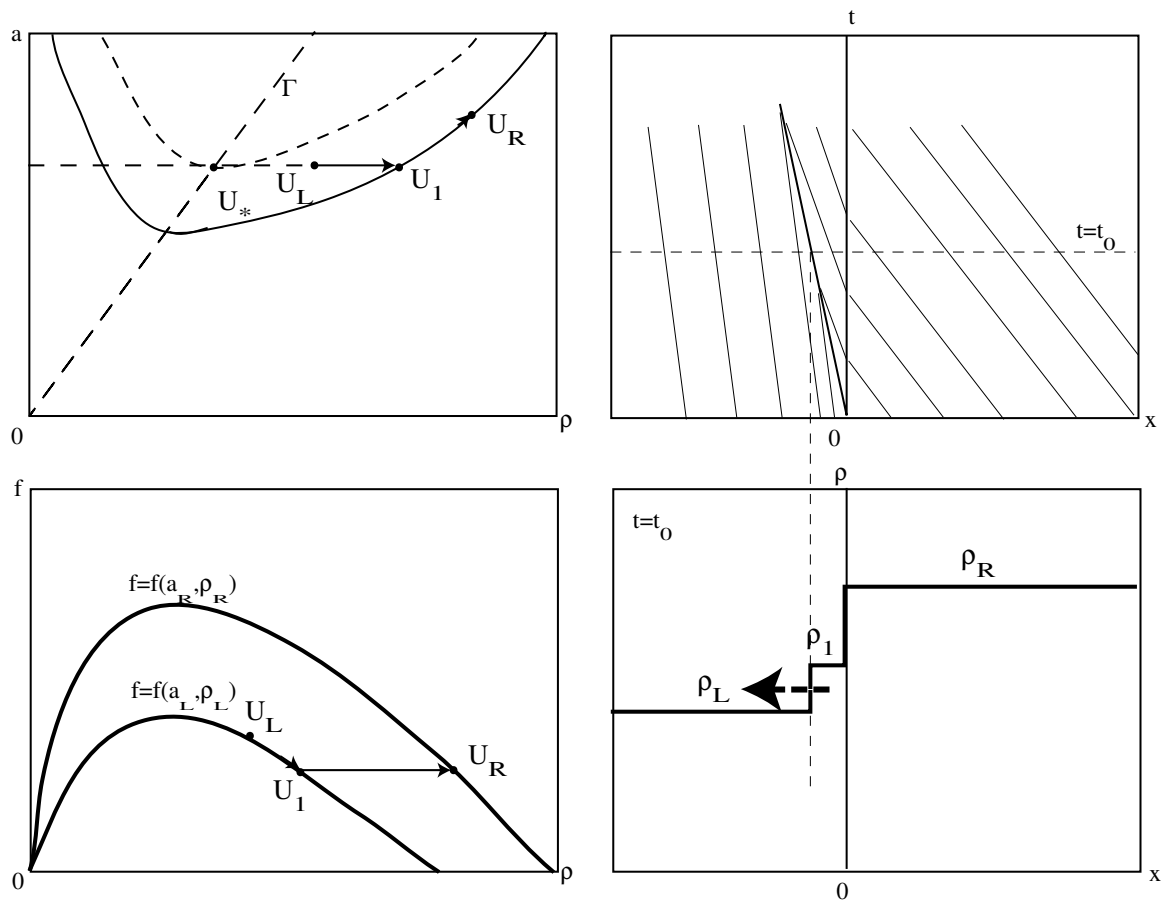


Figure 11: An example for wave solutions of type 8 for (5) with initial conditions (14)

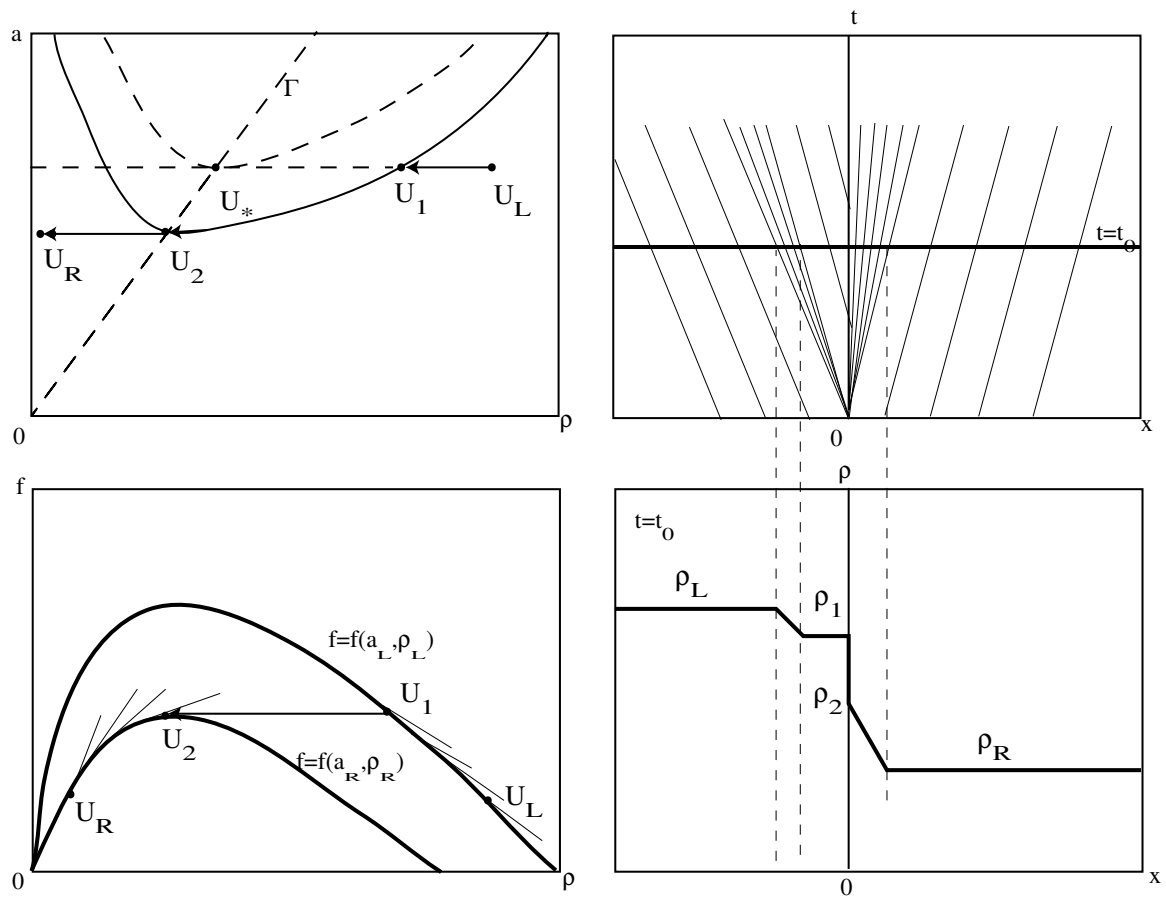


Figure 12: An example for wave solutions of type 9 for (5) with initial conditions (14)

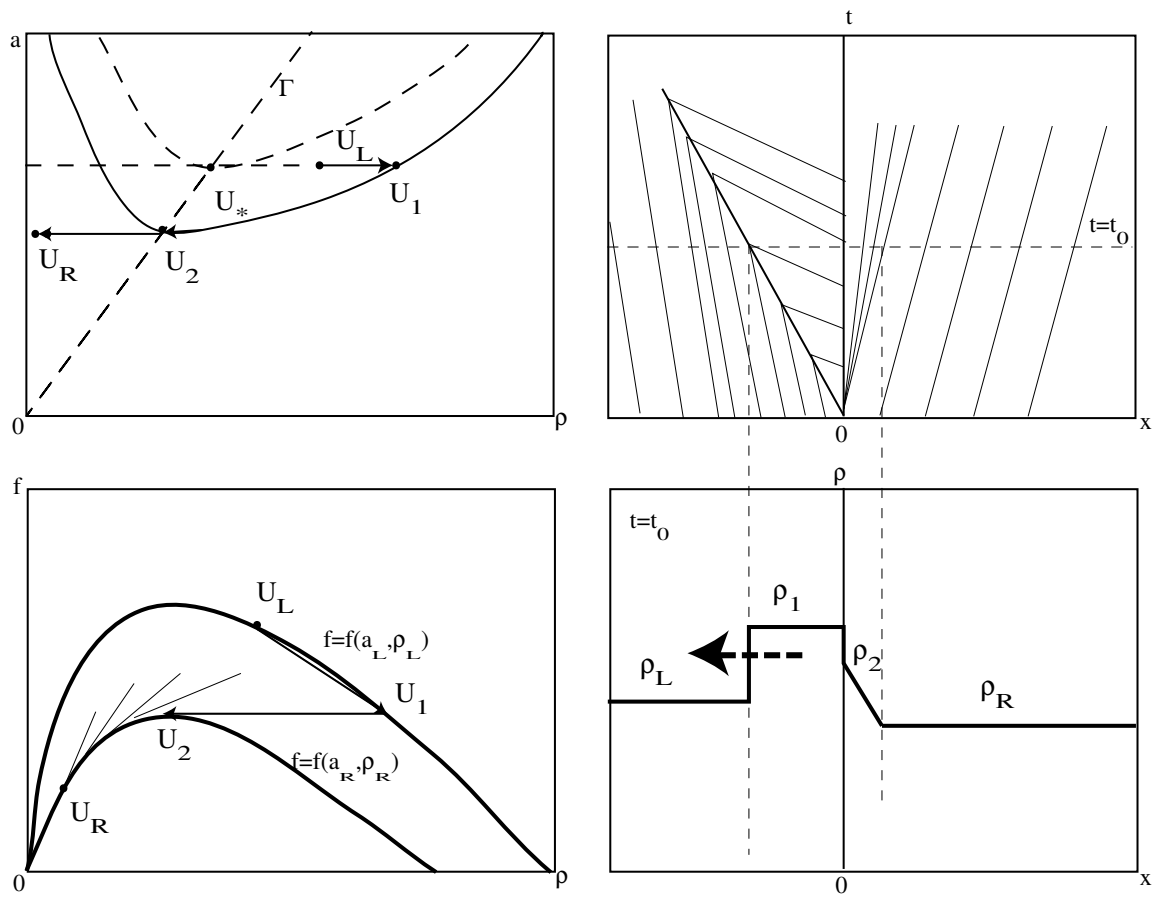


Figure 13: An example for wave solutions of type 10 for (5) with initial conditions (14)

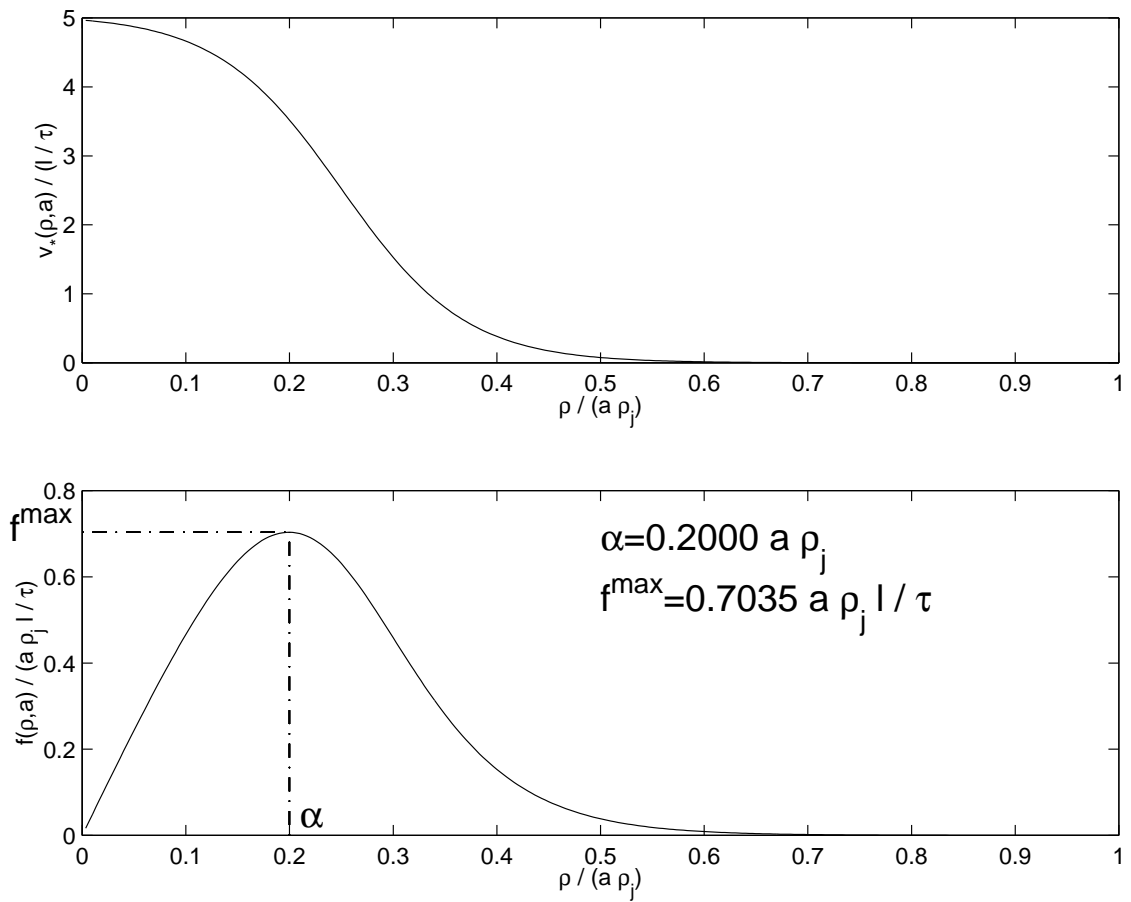


Figure 14: The Kerner-Konhäuser model of speed-density and flow-density relations

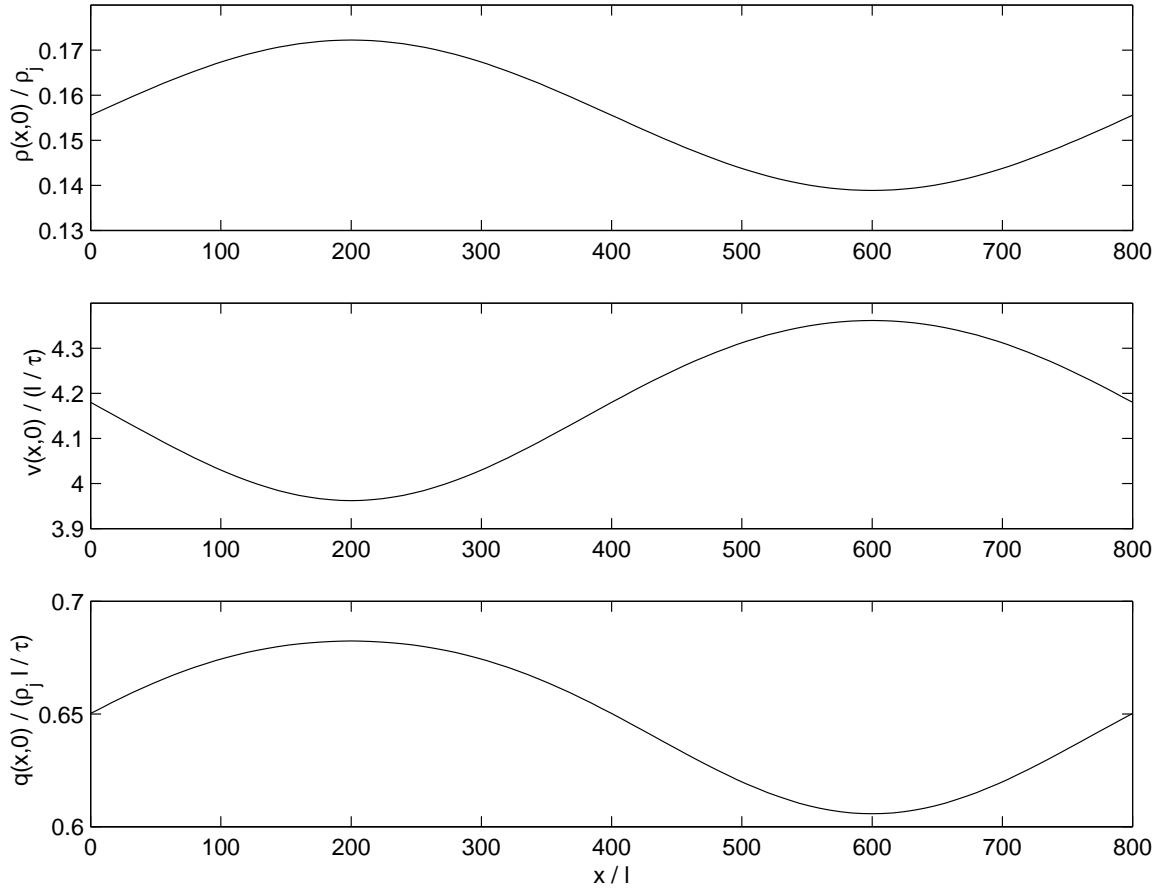


Figure 15: Initial condition (33) with  $\rho_h = 28$  veh/km and  $\Delta\rho_0 = 3$  veh/km

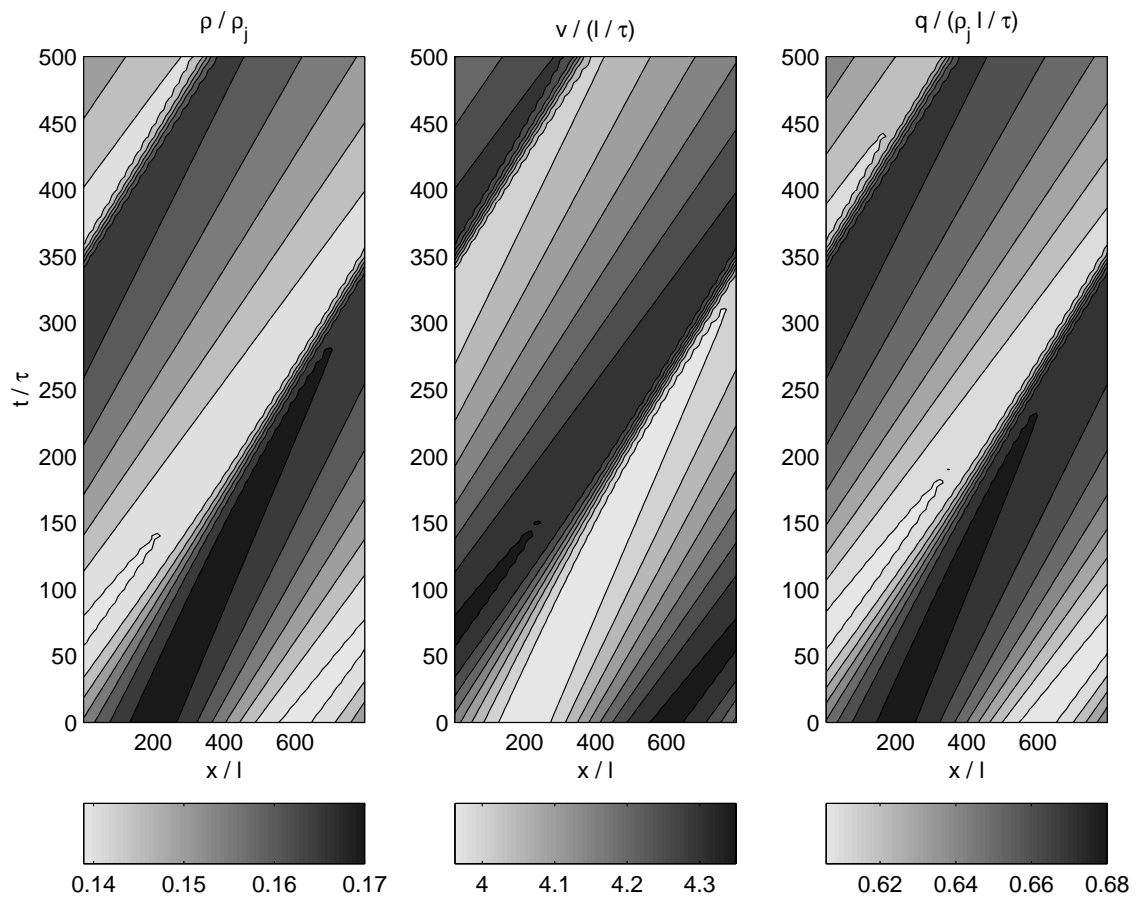


Figure 16: Solutions of the homogeneous LWR model with initial condition in **Figure 15**

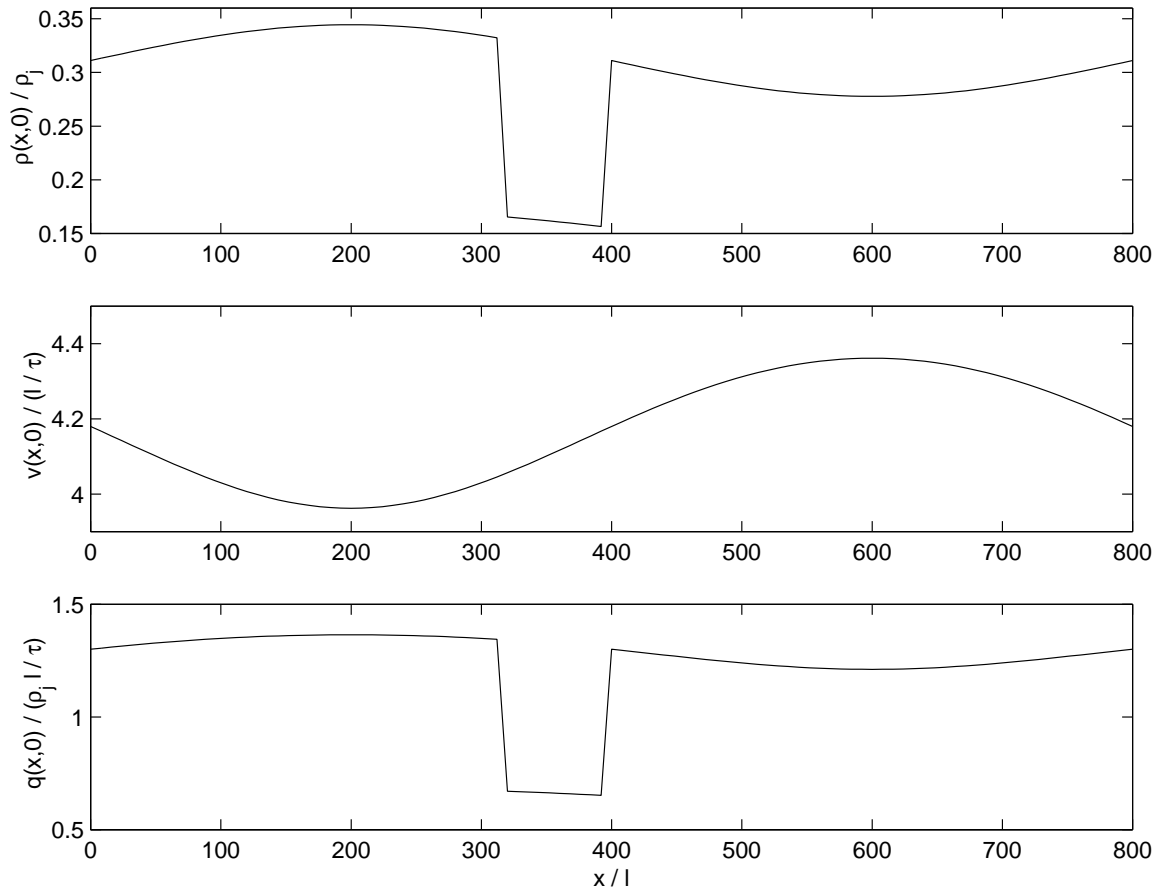


Figure 17: Initial condition (33) with  $\rho_h = 28$  veh/km/lane and  $\Delta\rho_0 = 3$  veh/km/lane

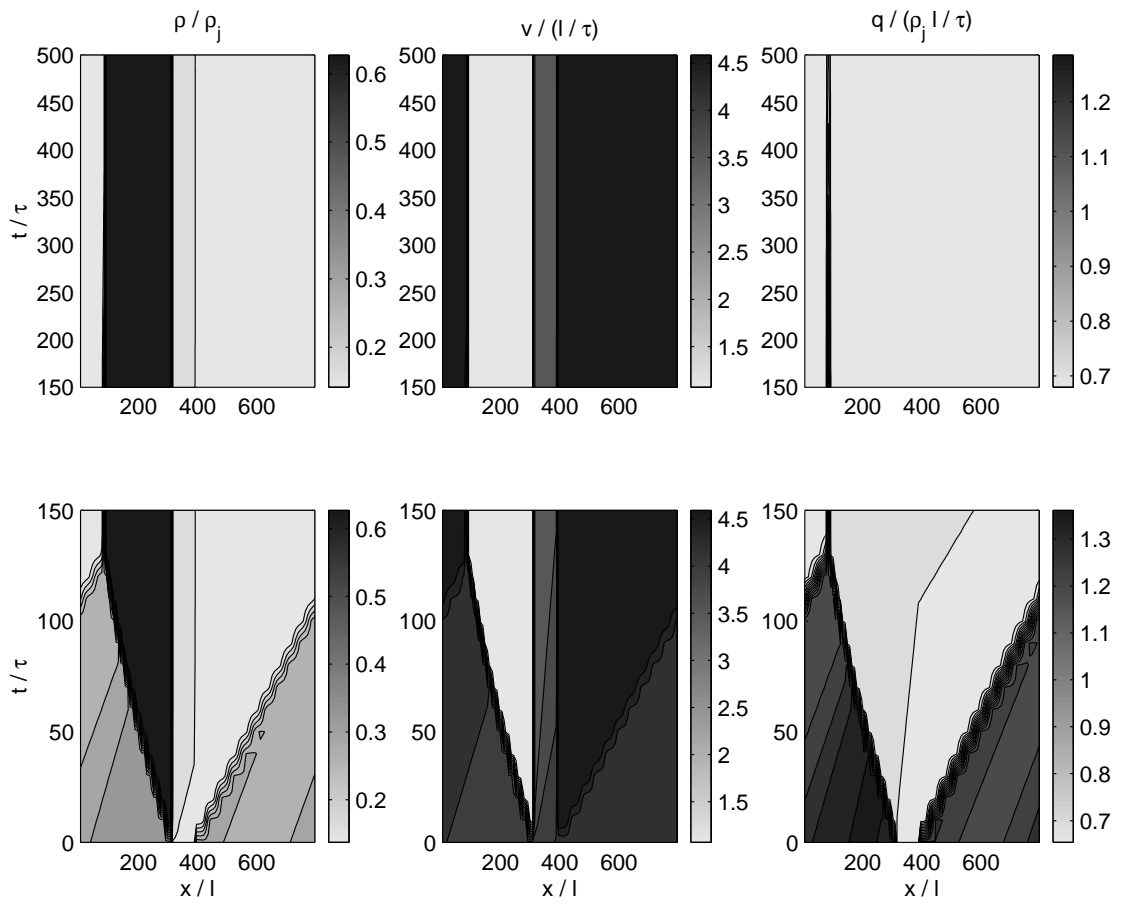


Figure 18: Solutions of the inhomogeneous LWR model with initial condition in **Figure 17**